

ZERO-BIAS CONDUCTANCE THROUGH SIDE-COUPLED DOUBLE QUANTUM DOTS

J. Bonča (janez.bonca@ijs.si)

*J. Stefan Institute, SI-1000 Ljubljana, and Department of Physics, FMF,
University of Ljubljana, SI-1000 Ljubljana, Slovenia*

R. Žitko (rok.zitko@ijs.si)

J. Stefan Institute, SI-1000 Ljubljana, Slovenia

Abstract. Low temperature zero-bias conductance through two side-coupled quantum dots is investigated using Wilson's numerical renormalization group technique. A low-temperature phase diagram is computed. Near the particle-hole symmetric point localized electrons form a spin-singlet associated with weak conductance. For weak inter-dot coupling we find enhanced conductance due to the two-stage Kondo effect when two electrons occupy quantum dots. When quantum dots are populated with a single electron, the system enters the Kondo regime with enhanced conductance. Analytical expressions for the width of the Kondo regime and the Kondo temperature in this regime are given.

Key words: Quantum dots, Kondo effect, Two-stage Kondo effect, Fano resonance

1. Introduction

The interplay between the Kondo effect (which involves coupling of the local moment to the conduction electrons) and the magnetic ordering of the moments has been studied in the context of bulk materials such as heavy-fermion metals (Jones and Varma, 1987). Recent advances in nanotechnology have enabled studies of transport through single as well as coupled quantum dots where Kondo physics and magnetic interactions play an important role at low temperatures. A double-dot system represents the simplest possible generalization of a single-dot system which has been extensively studied in the past. Recent experiments demonstrate that an extraordinary control over the physical properties, such as the intra-dot coupling, can be achieved in multiple dot systems (Jeong et al., 2001; Craig et al., 2004; Holleitner et al., 2002; Chen et al., 2004). This enables direct experimental investigations of the competition between the Kondo effect and the exchange interaction between localized moments on the dots. One manifestation of this competition is a two stage Kondo effect (Hofstetter



and Schoeller, 2003). Experimentally, it manifests itself as a sharp drop in the conductance vs. gate voltage (van der Wiel et al., 2002).

The Fano resonance is a characteristic of noninteracting electrons for which the shape of the Fano resonance can be analytically determined. However, the influence of interactions on the appearance of Fano resonances remains an open question. It has been recently observed in experiments on rings with embedded quantum dots (Kobayashi et al., 2002) and quantum wires with side-coupled dots (Kobayashi et al., 2004). The interplay between Fano and Kondo resonance was investigated using equation of motion (Bulka and Stefanski, 2001; Stefanski et al., 2004) and Slave boson techniques (Lara et al., 2004).

We study a double quantum dot (DQD) in a side-coupled configuration (Fig. 1), connected to a single conduction-electron channel. Similar systems were studied previously with different techniques, such as: non-crossing approximation (Kim and Hershfield, 2001), embedding technique (Apel et al., 2004), and slave-boson mean field theory (Kang et al., 2001; Lara et al., 2004). Numerical renormalization group (NRG) calculations were also performed recently (Cornaglia and Grepel, 2005), where only narrow regimes of enhanced conductance were found at low temperatures and no Fano resonances were reported. We will present a low-temperature phase diagram of a DQD as a function of intra-dot coupling strengths and gate-voltage potential indicating regions with enhanced conductance due to Kondo effect and regions of nearly zero conductance. In particular, when the intra-dot overlap is large and DQD occupancy is one, wide regimes of enhanced conductance as a function of gate-voltage exist at low temperatures due to Kondo effect, separated by the regimes where localized spins on DQD are antiferromagnetically (AFM) coupled. Kondo temperatures T_K follow a prediction based on the poor-man's scaling and Schrieffer-Wolff transformation. In the limit when the dot a is only weakly coupled, the system enters the "two stage" Kondo regime (Vojta et al., 2002a; Cornaglia and Grepel, 2005), where we again find a wide regime of enhanced conductivity under the condition that the high- and the low- Kondo temperatures (T_K and T_K^0 , respectively) are well separated and the temperature of the system T is in the interval $T_K^0 \ll T \ll T_K$.

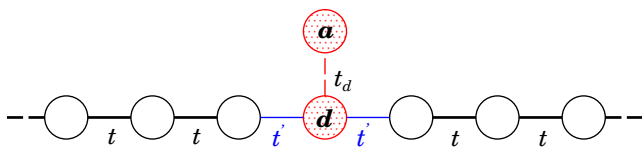


Figure 1. Side-coupled configuration of quantum dots.

2. Model and Method

The Hamiltonian that we study reads

$$\begin{aligned}
 H = & \delta(n_d - 1) + \delta(n_a - 1) - t_d \sum_{\sigma} \left(d_{\sigma}^{\dagger} a_{\sigma} + a_{\sigma}^{\dagger} d_{\sigma} \right) \\
 & + \frac{U}{2} (n_d - 1)^2 + \frac{U}{2} (n_a - 1)^2 \\
 & + \sum_{k\sigma} \epsilon_k c_{k\sigma}^{\dagger} c_{k\sigma} + \sum_{k\sigma} V_d(k) \left(c_{k\sigma}^{\dagger} d_{\sigma} + d_{\sigma}^{\dagger} c_{k\sigma} \right) \\
 & - J_{ad} \mathbf{S}_a \cdot \mathbf{S}_d,
 \end{aligned} \tag{1}$$

where $n_d = \sum_{\sigma} d_{\sigma}^{\dagger} d_{\sigma}$ and $n_a = \sum_{\sigma} a_{\sigma}^{\dagger} a_{\sigma}$. Operators d_{σ}^{\dagger} and a_{σ}^{\dagger} are creation operators for an electron with spin σ on site d or a . On-site energies of the dots are defined by $\epsilon = \delta - U/2$. For simplicity, we choose the on-site energies and Coulomb interactions to be equal on both dots. Coupling between the dots is described by the inter-dot tunnel coupling t_d . Dot d couples to both leads with equal hopping t' . Operator $c_{k\sigma}^{\dagger}$ creates a conduction band electron with momentum k , spin σ and energy $\epsilon_k = -D \cos k$, where $D = 2t$ is the half-bandwidth. Spin operator $\mathbf{S} = \sum_{s,s'} c_s^{\dagger} \vec{\sigma}_{s,s'} c_{s'}$ is defined using Pauli matrices and J_{ad} represents additional Heisenberg exchange interaction. The momentum-dependent hybridization function is $V_d(k) = -(2/\sqrt{N+1}) t' \sin k$, where N in the normalization factor is the number of conduction band states.

We use Meir-Wingreen's formula for conductance in the case of proportionate coupling (Meir and Wingreen, 1992), which is known to apply under very general conditions (for example, the system need not be in a Fermi-liquid ground state), with spectral functions obtained using the NRG technique (Wilson, 1975; Krishna-Murthy et al., 1980; Costi et al., 1994; Costi, 2001; Hofstetter, 2000). At zero temperature, the conductance is

$$G = G_0 \pi \Gamma \rho_d(0), \tag{2}$$

where $G_0 = 2e^2/h$, $\rho_d(\omega)$ is the local density of states of electrons on site d and $\Gamma/D = (t'/t)^2$.

The NRG technique consists of logarithmic discretization of the conduction band, mapping onto a one-dimensional chain, and iterative diagonalization of the resulting Hamiltonian (Wilson, 1975). Only low-energy part of the spectrum is kept after each iteration step; in our calculations we kept 1200 states, not counting spin degeneracies, using discretization parameter $\Lambda = 1.5$.

3. Strong intra-dot coupling

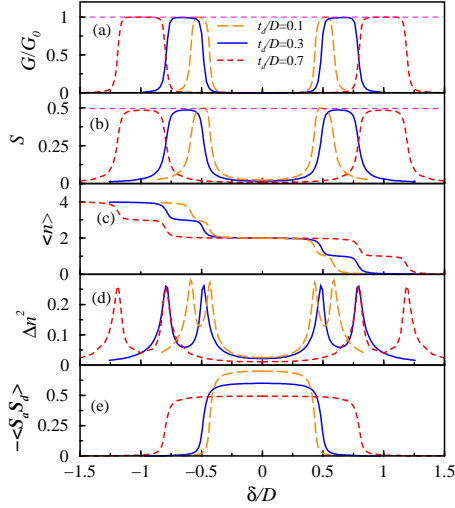


Figure 2. Conductance and correlation functions of DQD vs. δ . Besides different values of t_d , indicated in the figure, other parameters of the model are $\Gamma/D = 0.03$, $U/D = 1$ and $J_{ad} = 0$. Temperature T is chosen to be far below T_K , i.e. $T \ll T_K$.

In Fig. 2a we present conductance through a double quantum dot at different values of intra-dot couplings vs. δ . Due to formation of Kondo correlations, conductance is enhanced, reaching the unitary limit in a wide range of δ . Regimes of enhanced conductance appear in the intervals approximately given by $\delta_1 < |\delta| < \delta_2$, where $\delta_1 = t_d(2\sqrt{1 + (U/4t_d)^2} - 1)$ and $\delta_2 = (U/2 + t_d)$. These estimates were obtained from the lowest energies of states with one and two electrons on the isolated double quantum dot, *i.e.* $E_1 = U/2 - \delta - t_d$ and $E_2 = -2t_d\sqrt{1 + (U/4t_d)^2} + U/2$, respectively.

Using the above estimates we present a phase diagram in Fig. 3. In the gray region, called Kondo regime, with border lines given by $\delta_1(t_d), \delta_2(t_d)$, the Kondo effect is responsible for an enhanced conductance. Kondo plateaus in Fig. 2 fall in this regime. The Conductance is zero everywhere outside this region, except in the limit when $t_d \rightarrow 0$, where a two-stage Kondo effect two stage is responsible for enhanced conductance, as discussed further in the text.

To gain further physical insight, we focus on various correlation functions, defined within the DQD system. In Fig. 2b we show S , calculated from expectation value $\langle \mathbf{S}_{\text{tot}}^2 \rangle = S(S+1)$, where $\mathbf{S}_{\text{tot}} = \mathbf{S}_a + \mathbf{S}_d$ is the total spin operator. S reaches value $1/2$ in the Kondo regime where $G/G_0 = 1$. Enhanced conductance is thus followed by the local moment formation. This is further supported by the average double-dot occupancy $\langle n \rangle$, where $n = n_a + n_d$, which in the regime of enhanced conductivity approaches odd-integer values, *i.e.* $\langle n \rangle = 1$ and 3 (see Fig. 2c and 3). Transitions between regimes of nearly integer occupancies are rather sharp; they are visible as

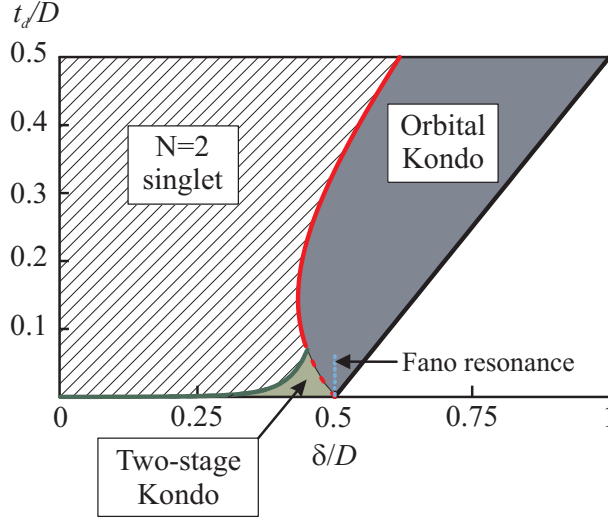


Figure 3. Phase diagram of a DQD for $U/D = 1$ and $J_{ad} = 0$, obtained using analytical estimates as given in the text. Grey areas represent Kondo regimes where $S \sim 1/2$, $\langle n \rangle \sim 1$, and $G/G_0 \sim 1$. In shaded area, called spin - singlet regime, where $S \sim 0$ and $\langle n \rangle \sim 2$, there is enhanced spin-spin correlation function, *i.e.* $\langle \mathbf{S}_a \cdot \mathbf{S}_d \rangle \lesssim -0.5$ and $G/G_0 \sim 0$. The two-stage Kondo regime is explained further in the text.

regions of enhanced charge fluctuations measured by $\Delta n^2 = \langle n^2 \rangle - \langle n \rangle^2$, as shown in Fig. 2d. Finally, we show in Fig. 2e spin-spin correlation function $\langle \mathbf{S}_a \cdot \mathbf{S}_d \rangle$. Its value is negative between two separated Kondo regimes where conductance approaches zero, *i.e.* for $-\delta_1 < \delta < \delta_1$, otherwise it is zero. This regime further coincides with $\langle n \rangle \sim 2$. Each dot thus becomes nearly singly occupied and spins on the two dots form a local singlet ($S=0$) due to effective exchange coupling $J_{\text{eff}} = 4t_d^2/U$.

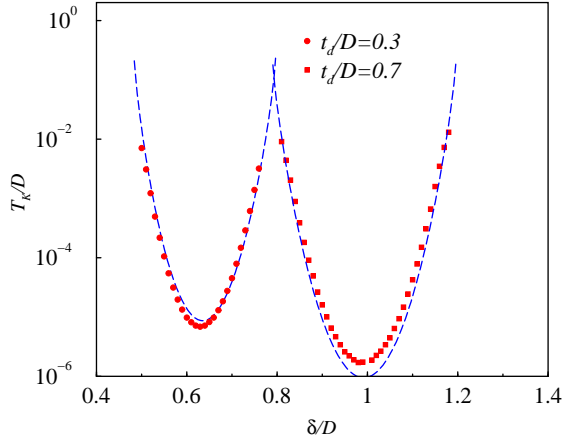


Figure 4. Kondo temperatures T_K vs. δ as measured from the widths of Kondo peaks obtained from NRG calculations (full circles and squares). Analytical estimate, Eq. 3, is shown using dashed lines. The rest of parameters are identical to those in Fig. 2.

In Fig. 4 we present Kondo temperatures T_K vs. δ extracted from the widths of Kondo peaks. Numerical results in the regime where $\langle n \rangle \sim 1$ and 3 fit the analytical expression obtained using the Schrieffer-Wolf transformation that projects out states with even electron occupancy and leads to an effective single quantum dot problem with renormalized parameters. We obtain

$$T_K = 0.182U\sqrt{\rho_0 J} \exp[-1/\rho_0 J] \quad (3)$$

with $\rho_0 J = \frac{2\Gamma}{\pi}(\alpha/|E_1| + \beta/|E_2 - E_1|)$, where $\alpha = 1/2$ and

$$\beta = \frac{\left(4t_d + U + \sqrt{16t_d^2 + U^2}\right)^2}{8\left(16t_d^2 + U\left(U + \sqrt{16t_d^2 + U^2}\right)\right)}. \quad (4)$$

The prefactor $0.182U$ in Eq. 3 is the effective bandwidth. The same effective bandwidth was used to obtain T_K of the Anderson model in the regime $U < D$ (Krishna-Murthy et al., 1980; Haldane, 1978).

4. Weak intra-dot coupling

We now turn to the *limit when* $t_d \rightarrow 0$. Unless otherwise specified, we choose the effective temperature T to be finite, *i.e.* $T \sim 10^{-9}D$, since calculations at much lower temperatures would be experimentally irrelevant. In this case one naively expects to obtain essentially identical conductance as in the single-dot case. As δ decreases below $\delta \sim U/2$, G/G_0 indeed follows result obtained for the single-dot case as shown in Fig. 5a. In the case of DQD, however, a sharp Fano resonance appears at $\delta = U/2$. This resonance coincides with the sudden jump in S , $\langle n \rangle$, as well as with the spike in Δn^2 , as shown in Figs 5b,c, and d, respectively. The Fano resonance is a consequence of a sudden charging of the nearly decoupled dot a , as its level ϵ crosses the chemical potential of the leads, *i.e.* at $\epsilon = 0$. Meanwhile, the electron density on the dot d remains a smooth function of δ , as seen from $\langle n_d \rangle$ in Fig 5c. With increasing t_d , the width of the resonance increases and at $t_d \gtrsim 0.1$, the resonance merges with the Kondo plateau and disappears (see Fig. 2a). The regime where the Fano resonance exists is also specified in the phase diagram, Fig. 3.

We now return to the description of the results presented in Fig. 5a in the regime where $\delta < U/2$. As δ further decreases, the system enters a regime of the two-stage Kondo effect (Cornaglia and Grempel, 2005). This region is defined by $J_{\text{eff}} < T_K$ (see also Fig. 5f), where T_K is the Kondo temperature, approximately given by the single quantum dot Kondo temperature, Eq. 3 with $\rho_0 J = \frac{2\Gamma}{\pi}(1/|\delta - U/2| + 1/|\delta + U/2|)$. This regime

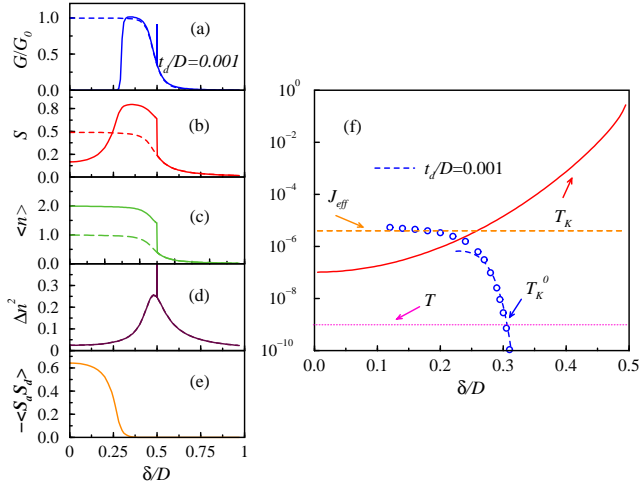


Figure 5. Conductance and correlation functions at $t_d/D = 0.001$ (a,...,e). Dashed lines represent in a) G/G_0 and in b) S of a single quantum dot with otherwise identical parameters. Dashed line in c) represents $\langle n_d \rangle$ of DQD. In f) a schematic plot of different temperatures and interactions is presented as explained in the text. NRG values of the gap in $\rho_d(\omega)$ at $\omega = 0$ and $T \ll T_K^0$ are presented with open circles. Values of J_{eff} and analytical results of T_K^0 are presented with dashed lines. For analytical estimates of T_K^0 $\alpha = 2.2$ was used. Other parameters of the model are $\Gamma/D = 0.03$, $U/D = 1$ and $J_{ad} = 0$.

is also indicated in the phase diagram, presented Fig. 4, where condition $J_{\text{eff}} = T_K$ was used to separate two-stage Kondo from the spin-singlet regime. Just below $\delta < U/2$, T falls in the interval, given by $T_K^0 \ll T \ll T_K$, where $T_K^0 \sim T_K \exp(-\alpha T_K/J_{\text{eff}})$ denotes the lower Kondo temperature, corresponding to the gap in the spectral density $\rho_d(\omega)$ at $\omega = 0$ and α is of the order of one (Cornaglia and Grempel, 2005). Note that NRG values of the gap in $\rho_d(\omega)$ (open circles), calculated at $T \ll T_K^0$, follow analytical results for $T_K^0(\delta)$ when $J_{\text{eff}} < T_K$, see Fig. 5f, while in the opposite regime, *i.e.* for $J_{\text{eff}} > T_K$, they approach J_{eff} .

As shown in Fig. 5a for $0.3D \lesssim \delta < U/2$, G/G_0 calculated at $T = 10^{-9}D$ follows results obtained in the single quantum dot case and approaches value 1. The spin quantum number S in Fig. 5b reaches the value $S \sim 0.8$, consistent with the result obtained for a system of two decoupled spin-1/2 particles, where $\langle \hat{S}^2 \rangle = 3/2$. This result is also in agreement with $\langle n \rangle \sim 2$ and the small value of the spin-spin correlation function $\langle \mathbf{S}_a \cdot \mathbf{S}_d \rangle$, presented in Fig. 5c and 5e respectively.

With further decreasing of δ , G/G_0 suddenly drops to zero at $\delta \lesssim 0.3D$. This sudden drop is approximately given by $T \lesssim T_K^0(\delta)$, see Figs. 5a and f. At this point the Kondo hole opens in $\rho_d(\omega)$ at $\omega = 0$, which in turn leads to a drop in the conductivity. The position of this sudden drop in terms of

δ is rather insensitive to the chosen T , as apparent from Fig. 5f.

Below $\delta \lesssim 0.25D$, which corresponds to the condition $J_{\text{eff}} \sim T_K(\delta)$, also presented in Fig. 5f, the system crosses over from the two stage Kondo regime to a regime where spins on DQD form a singlet. In this case S decreases and $\langle \mathbf{S}_a \cdot \mathbf{S}_d \rangle$ shows strong anti-ferromagnetic correlations, Figs. 5b and e. The lowest energy scale in the system is J_{eff} , which is supported by the observation that the size of the gap in $\rho(\omega)$ (open circles in Figs. 5f) is approximately given by J_{eff} .

5. Ferromagnetic coupling

In Fig 6 we present results of conductance and correlation functions for different values of the ferromagnetic exchange coupling J_{ad} , $t_d/D = 0.3$ and $U/D = 1$. At finite t_d and $J_{ad} = 0$ the ground state of an isolated DQD containing two electrons is a spin singlet state. At $J_{ad}^c/D = 2(\sqrt{4t_d^2 + U^2} - U) \sim 0.33$ spin singlet and triplet states become degenerate. With further increasing $J_{ad} > J_{ad}^c$ we expect formation of a $S = 1$ state in the regime when $\langle n \rangle \sim 2$. Since in this case $2S > K$ where $K = 1$ is the number of channels, this systems falls into a class where the spin on the DQD is not fully compensated by the conduction electrons (Vojta et al., 2002b; Hofstetter and Schoeller, 2003). Results at finite J_{ad} , presented in Fig 6, can be divided into two groups. For $J_{ad} < J_{ad}^c$ the main effect of increasing J_{ad} is seen as expansion of the $S = 1/2$ Kondo regime where $\langle n \rangle \sim 1$. For $J_{ad} > J_{ad}^c$, two Kondo plateaus appear, one associated with $S = 1/2$ Kondo regime and the other with $S = 1$ Kondo regime. In both cases conductance reaches unitary limit, while in the transition regime it drops to zero.

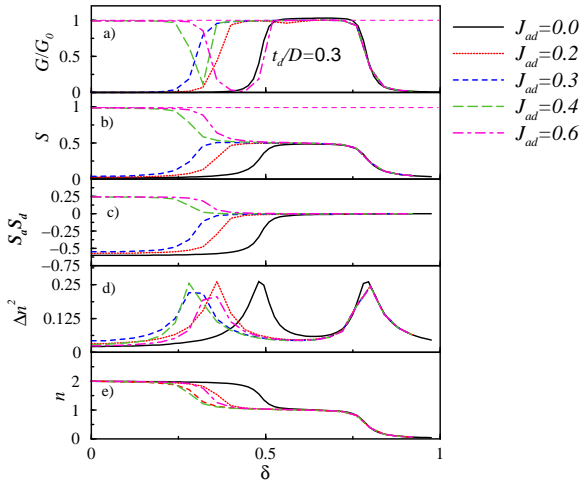


Figure 6. Conductance and correlation functions of DQD vs. δ for various values of J_{ad} and $t_d/D = 0.3$. Other parameters of the model are identical to those in Fig. 2. Temperature T is chosen to be far below T_K , i.e. $T \ll T_K$.

6. Conclusions

In this work we have explored different regimes of the side-coupled DQD. Conclusions can be summarized as follows: a) when quantum dots are *strongly coupled*, wide regions of enhanced, nearly unitary conductance exist due to the underlying Kondo physics. Analytical estimates for their positions, widths, as well as for the corresponding Kondo temperatures, are given and numerically verified. When two electrons occupy DQD, conductance is zero due to formation of the spin-singlet state which is effectively decoupled from the leads. b) In the limit when quantum dots are *weakly coupled* the Fano resonance appears in the valence fluctuation regime. Its width is enhanced as a consequence of interactions which should facilitate experimental observation. Unitary conductance exists when two electrons occupy DQD due to a two-stage Kondo effect as long as the temperature of the system is well below T_K and above T_K^0 . The experimental signature of the two-stage Kondo effect in weakly coupled regime should materialize through the inter-dot coupling sensitive width of the enhanced conductance vs. gate voltage.

When intra-dot ferromagnetic coupling exceeds a critical value, there is a phase transition from a spin-singlet, non-conducting regime to $S = 1$ Kondo regime where the spin on the DQD is under-screened but nevertheless the conductivity reaches the unitary limit.

Acknowledgements

Authors acknowledge useful discussions with A. Ramšak. We also acknowledge the financial support of the Slovenian Research Agency under grant P1-0044.

References

- Apel, V. M., Davidovich, M. A., Anda, E. V., Chiappe, G., and Busser, C. A. (2004) Effect of topology on the transport properties of two interacting dots, *Eur. Phys. J. B* **40**, 365.
- Bulka, B. R. and Stefanski, P. (2001) Fano and Kondo resonance in electronic current through nanodevices, *Phys. Rev. Lett.* **86**, 5128.
- Chen, J. C., Chang, A. M., and Melloch, M. R. (2004) Transition between Quantum States in a Parallel-Coupled Double Quantum Dot, *Phys. Rev. Lett.* **92**, 176801.
- Cornaglia, P. S. and Grempel, D. R. (2005) Strongly correlated regimes in a double quantum dot device, *Phys. Rev. B* **71**, 075305.
- Costi, T. A. (2001) Magnetotransport through a strongly interacting quantum dot, *Phys. Rev. B* **64**, 241310.
- Costi, T. A., Hewson, A. C., and Zlatic, V. (1994) Transport coefficients of the Anderson model via the numerical renormalization group, *J. Phys.: Condens. Matter* **6**, 2519.

- Craig, N. J., Taylor, J. M., Lester, E. A., Marcus, C. M., Hanson, M. P., and Gossard, A. C. (2004) Tunable Nonlocal Spin Control in a Coupled-Quantum Dot System, *Science* **304**, 565.
- Haldane, F. (1978) Theory of the Atomic Limit of the Anderson Model: I. Perturbation expansion re-examined, *J. Phys. C: Solid State Phys.* **11**, 5015.
- Hofstetter, W. (2000) Generalized Numerical Renormalization Group for Dynamical Quantities, *Phys. Rev. Lett.* **85**, 1508.
- Hofstetter, W. and Schoeller, H. (2003) Quantum Phase Transition in a Multilevel Dot, *Phys. Rev. Lett.* **88**, 016803.
- Holleitner, A. W., Blick, R. H., Hüttel, A. K., Eberl, K., and Kotthaus, J. P. (2002) Probing and Controlling the Bonds of an Artificial Molecule, *Science* **297**, 70.
- Jeong, H., Chang, A. M., and Melloch, M. R. (2001) The Kondo Effect in an Artificial Quantum Dot Molecules, *Science* **293**, 2221.
- Jones, B. A. and Varma, C. M. (1987) Study of Two Magnetic Impurities in a Fermi Gas, *Phys. Rev. Lett.* **58**, 843.
- Kang, K., Cho, S. Y., Kim, J.-J., and Shin, S.-C. (2001) Anti-Kondo resonance in transport through a quantum wire with a side-coupled quantum dot, *Phys. Rev. B* **63**, 113304.
- Kim, T.-S. and Hershfield, S. (2001) Suppression of current in transport through parallel double quantum dot, *Phys. Rev. B* **63**, 245326.
- Kobayashi, K., Aikawa, H., Katsumoto, S., and Iye, Y. (2002) Tuning of the Fano Effect through a Quantum Dot in an Aharonov-Bohm Interferometer, *Phys. Rev. Lett.* **88**, 256806.
- Kobayashi, K., Aikawa, H., Sano, A., Katsumoto, S., and Iye, Y. (2004) Fano resonance in a quantum wire with a side-coupled quantum dot, *Phys. Rev. B* **70**, 035319.
- Krishna-Murthy, H. R., Wilkins, J. W., and Wilson, K. G. (1980) Renormalization-group approach to the Anderson model of dilute magnetic alloys. I. Static properties for the symmetric case, *Phys. Rev. B* **21**, 1003.
- Lara, G. A., Orellana, P. A., Yanez, J. M., and Anda, E. V. (2004) Kondo effect in side coupled double quantum-dot molecule, cond-mat/0411661.
- Meir, Y. and Wingreen, N. S. (1992) Landauer formula for the current through an interacting electron region, *Phys. Rev. Lett.* **68**, 2512.
- Stefanski, P., Tagliacozzo, A., and Bulka, B. R. (2004) Fano versus Kondo Resonances in a Multilevel "Semiopen" Quantum Dot, *Phys. Rev. Lett.* **93**, 186805.
- van der Wiel, W. G., Franceschi, S. D., Elzerman, J. M., Tarucha, S., Kouwenhoven, L. P., Motohisa, J., Nakajima, F., and Fukui, T. (2002) Two-Stage Kondo Effect in a Quantum Dot at a High Magnetic Field, *Phys. Rev. Lett.* **88**, 126803.
- Vojta, M., Bulla, R., and Hofstetter, W. (2002)a Quantum phase transitions in models of coupled magnetic impurities, *Phys. Rev. B* **65**, 140405.
- Vojta, M., Bulla, R., and Hofstetter, W. (2002)b Quantum phase transitions in models of coupled magnetic impurities, *Phys. Rev. B* **65**, 140405(R).
- Wilson, K. G. (1975) The renormalization group: Critical phenomena and the Kondo problem, *Rev. Mod. Phys.* **47**, 773.